Statistica Sinica **17**(2007), 15-41

FREQUENCY ANALYSIS OF CHAOTIC INTERMITTENCY MAPS WITH SLOWLY DECAYING CORRELATIONS

R. J. Bhansali and M. P. Holland

University of Liverpool and University of Exeter

Abstract: Established stochastic models for discrete-time long-memory processes are linear and Gaussian, and commonly require that the dth fractional-difference of the process has short memory $0 < d \leq 0.5$; if $-0.5 < d < 0$, the process is said to have an intermediate memory. Chaotic intermittency maps provide alternative nonlinear, non-Gaussian models for both classes of processes. An asymptotic expression for the rate at which the correlations of symmetric cusp map decay is developed, and the class of extended symmetric cusp maps is introduced. The small-frequency asymptotics of the polynomial, cusp and logarithmic maps are investigated, and it is shown that these maps can produce spectra with $d = 0.5$ on the one hand, $d = 0$ on the other, and yet the corresponding processes are stationary and have long-memory. Asymptotic expressions are derived for studying the bias of the small-frequency periodogram ordinates with these maps. Finite sample behaviour is examined in a simulation study.

Key words and phrases: Fractional differencing, long memory, nonlinear time series; non-Gaussian time series, periodogram, small frequency asymptotics, spectral density function.

1. Introduction

The class of stationary processes admitting long-memory has received much attention lately, see Doukhan, Oppenheim and Taqqu (2002), Rangrajan and Ding (2003), and the papers therein. Many of the suggested stochastic long-memory models are, however, linear and, following Box, Jenkins and Reinsel (1994), typically envisage that a fractionally-differenced process has short-memory.

Thus, let $\{w_t\}$, $t = \ldots, -1, 0, 1, \ldots$, denote a weakly stationary process with mean $\eta_w = E(w_t)$, covariance function $R_{ww}(u) = E[\{w_t - \eta_w\}\{w_{t+u} - \eta_w\}]$, correlation function $r_{ww}(u) = R_{ww}(u)/R_{ww}(0)$, and spectral density function

$$f_{ww}(\lambda) = (2\pi)^{-1} \sum_{u=-\infty}^{\infty} R_{ww}(u) \exp(-iu\lambda). \tag{1}$$

Also, for two functions h and g defined in the neighbourhood of a point a, let $h(\lambda) \sim g(\lambda)$ as $\lambda \to a$ denote the fact that $h(\lambda)/g(\lambda) \to 1$ as $\lambda \to a$.

The existing long-memory models usually specify that the dth fractional difference process

$$x_t = (1 - z)^d w_t, \tag{2}$$

where z denotes the backshift operator $z^j w_t = w_{t-j}$, has exponentially decaying correlations, $0 < d < 0.5$.

The stationary process $\{w_t\}$ so defined admits long-memory as follows:

(a) the correlations decrease to zero at a polynomial rate, $r_{ww}(u) \sim Bu^{2d-1}$ as $u \to \infty$, where B denotes a bounded constant;
(b) the covariance function R_{ww} is not summable:

$$\sum_{u=-\infty}^{\infty} R_{ww}(u) = \infty; \tag{3}$$

(c) the spectral density function f_{ww} has a singularity at the origin,

$$f_{ww}(\lambda) \sim |\lambda|^{-2d} \Delta(1/|\lambda|) \quad \text{as} \quad \lambda \to 0, \tag{4}$$

where $\Delta(\lambda)$ is a bounded slowly-varying function at infinity.

For $-0.5 < d < 0$, an intermediate-memory process with an absolutely-summable covariance function is defined; see Mcleod (1998).

Chaotic intermittency maps provide a new and an entirely different approach to long-memory. These maps are typically non-linear and non-Gaussian and possess three important properties: first, whereas the Tent, Bernoulli and associated classical maps possess short memory, the correlations of intermittency maps decay at a sub-exponential rate; second, their invariant density χ can approach infinity near the origin at a sub-exponential rate; third, the orbit of these maps displays intermittent chaos, meaning it switches between laminar and chaotic regions. Indeed, the phenomenon of intermittency motivating this class of maps has been widely observed, see Barndorff-Nielsen (2001) among others.

Bhansali, Holland and Kokoszka (2005) have developed a formal definition of the intermittent family of maps and applied this definition for distinguishing between the Polynomial, Logarithmic, Generalised Polynomial- Logarithmic and Cusp maps. The asymptotic rates of the decay of correlations for these maps are also discussed and it is noted that, whereas an exact expression for the decay rate is now known for the polynomial maps, only an upper bound is available for the other three. Also, Bhansali, Holland and Kokoszka (2006) investigate, by a simulation study, the empirical behaviour of the estimated correlations and invariant densities for the polynomial, logarithmic and asymmetric cusp maps.

In this paper, we focus on frequency domain properties of intermittency maps. In Section 3, an asymptotic expression for the rate of decay of correlations for the symmetric cusp map is developed by connecting this rate to the recurrence properties of the map. Moreover, the class of extended symmetric cusp maps is also introduced and related to polynomial maps. Asymptotic expressions for the rate at which the correlations of logarithmic and generalised polynomial-logarithmic maps decay are also given in this section.

The asymptotics of the spectral density functions of these maps near the origin are examined in Section 4. We show, in particular, that the spectral densities of the symmetric cusp map and polynomial map with $\alpha = 0.5$ behave like a logarithmic function near the origin, $f_{ww}(\lambda) \sim B \log(|\lambda|)$, as $|\lambda| \to 0$. An interpretation of this result is that, although $d = 0$ for these two maps, they display long-memory, since their correlations decay like a harmonic series. For the logarithmic map, by contrast, we show that $f_{ww}(\lambda) \sim B|\lambda|^{-1}|\log(|1/\lambda|)$ as $|\lambda| \to 0$, and hence, although $d = 0.5$ for this map, it defines a stationary process. Our results thus enable the behaviour of long-memory time series to be studied at the boundary of the values of d specified in (4), and show by example that, unless the slowly-varying function Δ occurring there is bounded, the hypothesis that $d = 0$ need not imply that the process has short memory. Conversely, $d = 0.5$ need not imply that the process is non-stationary.

On the assumption that a realization of T consecutive observations from an intermittency map is observed, with the initial value obtained from its invariant density, some of the asymptotic sampling properties of the low-frequency periodogram ordinates for these maps are examined in Section 5 as $T \to \infty$. The results here generalise and extend those of Hurvich and Beltrao (1993), who earlier considered a similar problem but assumed that (2) holds; see also Robinson (1995).

Section 6 presents simulation results examining the empirical properties of the low-frequency periodogram ordinates for the polynomial, logarithmic and symmetric cusp maps. The results here complement the earlier 'time domain' results of Bhansali, Holland and Kokoszka (2005), and throw light on how the standard GPH and related methods for estimating the long-memory parameter might perform in the non-standard settings arising in these maps.

The intermittency maps we consider were originally introduced for characterizing transition to turbulence, see Schuster and Just (1999); in these maps, long-memory is an intrinsic property of the models describing this transition. A different form of intermittency arises when modelling the sporadic bursts in high-pass filtered time series, see Frisch (1996); Gao, Anh, Heyde and Tieng (2001)

consider Gaussian processes exhibiting this particular form of intermittency as well as long-memory.

Processes exhibiting a boundary behaviour of the type discussed in this paper could also arise when an instantaneous polynomial transformation is applied to a Gaussian long-memory process. Giraitis and Taqqu (1999) have investigated the asymptotic distribution of the Whittle-likelihood estimators of 'spectral' parameters in this situation. For the maps we consider, however, this boundary behaviour arises directly when modelling intermittency.

Martin and Eccleston (1992) and Martin and Walker (1997) are additional references related to our work. These authors show that for the process with exact harmonic correlation structure, $r(n) = \rho/n$, $(n \neq 0)$, where $0 \leq \rho \leq (2\log 2)^{-1}$ is a bounded constant, the spectral density f_{ww} also diverges to ∞ as $\lambda \to 0$, at a logarithmic rate. However, although motivated by an actual application, see Russell and Eccleston (1987), these studies do not provide an explicit example of a stationary process giving rise to this correlation structure.

2. Chaotic Intermittency Maps

2.1. General properties

By a map time series we mean a deterministic sequence, $\{w_t,\, t \in \mathbb{N}\}$, generated by iteratively applying a one-dimensional map of the following form:

$$w_{t+1} = \zeta(w_t)\,(t \in \mathbb{N}), \tag{5}$$

where $\zeta : J \to J$ is a non-linear map (function), J denotes a closed interval of the real line $\mathbb{R}$, $\mathbb{N}$ is the set of non-negative integers, and w_0 specifies the *initial condition*.

If the map ζ is ergodic and admits an invariant density, χ say, then provided the initial condition w_0 is a random number from this invariant density, $\{w_t\}$ defines a strictly stationary stochastic process, see Berliner (1992), among others.

Denote the first derivative of ζ by ζ'. A fixed point, $\tilde{w}$ say, is defined as a solution of the equation $\zeta(\tilde{w}) = \tilde{w}$. We say that $\tilde{w}$ is an attracting fixed point if $|\zeta'(\tilde{w})| < 1$, a repelling fixed point if $|\zeta'(\tilde{w})| > 1$, and an indifferent, or a neutral, fixed point if $|\zeta'(\tilde{w})| = 1$.

An important property of intermittency maps is that they admit a neutral fixed point, see Bhansali, Holland and Kokoszka (2005). Let $\mathcal{H}$ denote the class of all Hölder continuous functions. If $\varphi \in \mathcal{H}$ and if ζ is ergodic and admits an invariant density χ, the expectation and variance of $\varphi(w_n)$ are given by, for all $n \in \mathbb{N}$:

$$E\big\{\varphi(w_n)\big\} = \int_J \varphi(w)\chi(w)dw, \tag{6}$$

$$V\{\varphi(w_n)\} = E\{\varphi(w_n)^2\} - (E\{\varphi(w_n)\})^2. \tag{7}$$

Similarly, for all $\varphi, \psi \in \mathcal{H}$ and $n \in \mathbb{N}$, the covariance between $\varphi(w_n)$ and $\psi(w_0)$ is

$$\begin{aligned} R_{\varphi,\psi}(n) &= E\{\varphi(w_n)\psi(w_0)\} - E\{\varphi(w_n)\}E\{\psi(w_0)\} \\ &= \int_J \varphi(\zeta^n(w))\psi(w)\chi(w)dw - \int_J \varphi(w)\chi(w)dw \int_J \psi(w)\chi(w)dw. \end{aligned} \tag{8}$$

For $\psi(w) = \varphi(w) = w$, $R_{\varphi,\psi}(n) = R_{ww}(n)$ is the autocovariance function of the process $\{w_t, t \in \mathbb{N}\}$.

As is well known, the Lyapunov exponent gives a measure of how chaotic a map is, how sensitive the orbit $\{w_n, n \in \mathbb{N}\}$ is to the initial condition w_0. For a point w it is defined by

$$L(w) = \lim_{n\to\infty} \frac{1}{n} \log |(\zeta^n)'(w)|. \tag{9}$$

Positive Lyapunov exponents imply that the map is chaotic.

An intermittency map ζ, however, displays chaotic behaviour on a set $A \subset J$, not necessarily over the whole of J. Hence, the Lyapunov exponent for an intermittency map could either vanish, which is so with the Farey map defined later by (17) or, as with the symmetric cusp map defined by (14), it could exceed 0.

The Lyapunov exponent does not provide any information on the long (or short) memory properties of a map. As an example, consider the map $\chi_\beta(w) = \beta w \,(\mathrm{mod} 1)$ with Lyupanov exponent $\log \beta$, while for all $\beta > 1$, it has short memory.

The rate of decay of correlations is however connected to the recurrence properties of a map. Suppose that $w_0 \in C$, where $C \subset J$ is some fixed interval. The recurrence property that is of interest is the time, $T_C(w_0)$ say, for the orbit to return to C for the first time, having started from within this interval. To this end, let

$$H_C(n) = P(T_C(w_0) \le n \mid \ w_0 \in C) \quad (n = 1, 2, \ldots) \tag{10}$$

denote the distribution function of $T_C(w_0)$. Clearly, $H_C(n) \to 1$, as $n \to \infty$. For a short memory map, $H_C(n) \to 1$ at an exponential rate as $n \to \infty$ for every $C \subset J$. By contrast, for an intermittency map there may exist sub-intervals C for which this rate of decay is sub-exponential.

We summarise below some basic statistical properties of the three different classes of intermittency maps, namely the *Polynomial, Cusp* and *Logarithmic* maps, see Bhansali, Holland and Kokoszka (2005) for further details.

2.2. Polynomial maps

This class of maps is defined for $J = [0, 1]$ by

$$\zeta_\alpha(w) = \begin{cases} w(1 + 2^\alpha w^\alpha) & \text{if } 0 \le w \le \frac{1}{2}, \\ 2w - 1 & \text{if } \frac{1}{2} < w \le 1, \end{cases} \tag{11}$$

where $\alpha > 0$ (see Liverani, Saussol and Vaienti (1999) and Young (1999)).

When $\alpha \in (0, 1)$, this map is ergodic and admits an invariant density χ_α. An explicit expression for χ_α is unknown, but it is known that

$$\chi_\alpha(w) = \frac{V_\alpha(w)}{w^\alpha}, \tag{12}$$

where $V_\alpha(w)$ depends on the value of α and, for each fixed α, it is a piecewise continuous, uniformly bounded function of w which is also bounded away from zero.

2.3. Cusp maps

Balakrishnan, Nicolis and Nicolis (1997, 2001) have investigated this class. Two different maps are considered, namely an *asymmetric* cusp map and a *symmetric* cusp map. The former is defined for $J = [-1, 1]$ by

$$\zeta_C(w) = \begin{cases} 1 - 2\sqrt{(-w)} & \text{if } -1 \le w \le 0, \\ 2\sqrt{(w)} - 1 & \text{if } 0 < w \le 1. \end{cases} \tag{13}$$

Its invariant density, χ_C, coincides with that of a uniform distribution on $J = [-1, 1]$. The symmetric cusp map is defined by, with $J = [-1, 1]$,

$$\zeta_S(w) = 1 - 2\sqrt{|w|}. \tag{14}$$

The map displays intermittent behaviour because it has a neutral fixed point at $w = -1$. It is also ergodic with a triangular invariant density (see Balakrishnan, Nicolis and Nicolis (1997)),

$$\chi_S(w) = \frac{1}{2}(1 - w), \tag{15}$$

and the Lyapunov exponent is $1/2$ for almost all $w \in J$.

It is possible to generalize both symmetric and asymmetric cusp maps so as to incorporate other types of singularities and neutral fixed points. One such

generalization is the family of *extended symmetric cusp maps* defined over $J = [-1, 1]$, and parametrised by two parameters, $\tau > 0, \theta \in (0, 1)$:

$$\zeta_{\tau,\theta}(w) = \begin{cases} w + (w+1)^{1+\tau}, & -1 \le w \le -1+\delta, \\ \tilde{\zeta}(w), & -1+\delta < w \le -\delta, \\ 1 - |w|^{\theta}, & -\delta < w \le 0, \\ \zeta_{\tau,\theta}(-w), & 0 < w \le 1, \end{cases} \tag{16}$$

where $\delta > 0$ is a small constant, $\tilde{\zeta}(w)$ is chosen to be a uniformly expanding (everywhere sensitive dependent) map on $[-1+\delta, -\delta]$, and such that the map $\zeta_{\tau,\theta}$ is continuous on J. For example, $\tilde{\zeta}_{\tau,\theta}(w)$ can be chosen to be the linear map on $[-1-\delta, -\delta]$ given by

$$\tilde{\zeta}(w) = \left(\frac{2 - \delta - \delta^{1+\tau} - \delta^{\theta}}{1 - 2\delta} \right) (w + 1 - \delta) - 1 + \delta + \delta^{1+\tau}.$$

The laminar region of the map is $J_\delta = [-1, -1+\delta]$, τ controls the expected time spent in J_δ, assuming that the initial condition $w_0 \in J_\delta$, while θ controls the expected time spent in J_δ, assuming the initial condition is outside the laminar region.

When $\tau\theta > 1$ the map is not ergodic. For $\tau\theta < 1$ a smooth invariant density does exist, although an explicit formula for it is unknown.

When $\theta = 1$, the recurrence properties of the map are related to those of the polynomial maps.

The Farey map is an additional example of a cusp map. It has been considered, see Pronzato, Wynn and Zhigliavsky (2001), in connection with certain line search algorithms and, for $J = [0, 1]$,

$$\zeta_F(w) = \begin{cases} \frac{w}{1-w} & \text{if} \quad 0 \le w \le \frac{1}{2}, \\ \frac{1-w}{w} & \text{if} \quad \frac{1}{2} < w \le 1. \end{cases} \tag{17}$$

This map has a neutral fixed point at $w = 0$ and it is ergodic. The invariant density is however improper, $\chi_F(w) \propto w^{-1}$. A normalized version of $\chi_F(w)$ coincides with the density of a degenerate Dirac distribution. An equivalence between the Farey map and the polynomial map with $\alpha = 1$ can be established by noting that, up to terms of second order, a Taylor expansion gives $\zeta_F(w) = w + w^2 + O(w^3)$ as $w \to 0$ which, on ignoring $O(w^3)$ terms, agrees with the definition of the polynomial map with $\alpha = 1$, up to a multiplying constant.

An equivalence between the Farey map and the modified cusp map, with $(\tau, \theta) = (1, 1)$, may also be established by an analogous argument.

2.4. Logarithmic maps

This class of intermittency maps was introduced by Holland (2005) as a generalisation of the polynomial map. It is defined on $J = [0, 1]$ by

$$\zeta_\beta(w) = \begin{cases} w\left[1 + Y(\beta) w (-\log w)^{1+\beta}\right] & \text{if} \quad 0 \le w \le \frac{1}{2}, \\ 2w - 1 & \text{if} \quad \frac{1}{2} < w \le 1, \end{cases} \tag{18}$$

where $Y(\beta) = 2(\log 2)^{-(1+\beta)}$ is chosen to ensure that $\lim_{w \to 1/2^-} \zeta_\beta(w) = 1$, β a parameter of the map.

The map is ergodic for all $\beta \in (0, 2\log 2 - 1)$, and its invariant density takes the following form on $(0, 1/2)$:

$$\chi_\beta(w) = \frac{V_\beta(w)}{w \log(\frac{1}{w})^{\beta+1}} \quad \forall\, w \in J. \tag{19}$$

Here $V_\beta(w)$ depends on β and, for each fixed β, it is a uniformly bounded piecewise continuous function that is also bounded away from zero; on $[1/2, 1]$, the invariant density is a bounded piecewise continuous function.

It is also possible to combine the polynomial and logarithmic maps by defining the generalised polynomial-logarithmic maps as

$$\zeta_\gamma(w) = \begin{cases} w\left[1 + Y(\gamma) w^\gamma L(w)\right] & \text{if} \quad 0 \le w \le \frac{1}{2}, \\ 2w - 1 & \text{if} \quad \frac{1}{2} < w \le 1, \end{cases} \tag{20}$$

where $\gamma > 0$, $Y(\gamma) = 2^\gamma / L(1/2)$, and $L(1/w)$ is slowly varying function at ∞ that is twice differentiable for all $w \in [C, \infty]$, C a bounded constant, see Bhansali, Holland and Kokoszka (2006).

3. Asymptotic Rates of Correlation Decay

Let

$$r_{\varphi,\psi}(n) = R_{\varphi,\psi}(n) / \sqrt{\left\{V\left\{\varphi(w_n)\right\} V\left\{\psi(w_0)\right\}\right\}} \tag{21}$$

denote the cross-correlation function between $\varphi(w_n)$ and $\psi(w_0)$, $n = 0, \pm 1, \ldots$, where $\varphi(w_n)$ and $\psi(w_n)$ are two Hölder continuous functions of the map time series $\{w_t\}$. In this section, we derive asymptotic results for the rate at which $r_{\varphi,\psi}(n)$ decreases to 0 as $n \to \infty$, for the symmetric cusp and the extended

symmetric cusp maps, and relate these rates to the corresponding rates for the polynomial map. In addition, we also examine the correlation decay rate for the logarithmic and the generalized polynomial-logarithmic maps.

3.1. Polynomial maps

For the map (11), the asymptotic decay of $r_{\varphi,\psi}$ has been studied by several authors, see Bhansali, Holland and Kokoszka (2005), and a general result is due to Sarig (2002) and Gouëzel (2004b), who show that for $\varphi, \psi \in \mathcal{H}$,

$$\lim_{n\to\infty} n^{\frac{1}{\alpha-1}} r_{\varphi,\psi}(n) = U, \tag{22}$$

where U is a constant. Hence, like the fractionally-differenced time series defined by (2), the correlations for the polynomial map decay at a polynomial rate.

Indeed we may set $d = 1 - (2\alpha)^{-1}$, and for $\alpha \in (0.5, 1.0)$ the map admits long-memory, while for $\alpha \in (1/3, 0.5)$ the map admits intermediate memory. If $[x]$ denotes the integer part of a real number x, for $\alpha \in (0, 1/3]$ the correlations behave asymptotically like that of a time series whose p-th difference, $p = [1-(2\alpha)^{-1}]$, is a fractionally-differenced process. By contrast, for $\alpha = 0.5$ the correlations decay harmonically, $r_{\varphi,\psi}(n) \sim Bn^{-1}$, for some $B > 0$ and, although $d = 0$, the series still displays long memory.

3.2. Cusp maps

Exact expressions for the mean, variance and the first correlation coefficient of the symmetric cusp map may be written down from the known invariant density. We have, for all t, $E(w_t) = -(1/3)$, $\mathrm{Var}(w_t) = R_{ww}(0) = (2/9)$, $\mathrm{cov}(w_t, w_{t+1}) = R_{ww}(1) = (8/63)$, $\mathrm{corr}(w_t, w_{t+1}) = (4/7)$. The evaluation of $r_{ww}(n)$ for $n \geq 2$ is not straightforward. The following theorem gives the asymptotic rate of decay of the covariances $R_{ww}(n)$ for the symmetric cusp map. A proof of this theorem is given in the *Appendix*.

Theorem 3.1. *For the symmetric cusp map,* $R_{ww}(n) = 4/(9n) + o(1/n)$.

By a study of the recurrence properties of the extended symmetric cusp maps, the following theorem can be established. A proof of this theorem is omitted, since it is similar to that for the symmetric cusp map but in a slightly more general setting.

Theorem 3.2. *The family of extended symmetric cusp maps* $\zeta_{\tau,\theta}$*, possesses the following properties:*

(a) *For* $\tau\theta < 1$, $\zeta_{\tau,\theta}$ *admits an absolutely continuous invariant probability measure* $\mu_{\tau,\theta}$ *that is ergodic;*
(b) *for all Hölder continuous functions* φ, ψ*, as* $n \to \infty$, $R_{\varphi,\psi}(n) = O\left(n^{1-1/(\tau\theta)}\right)$;
(c) *there exists a constant* $C_{\tau,\theta}$ *such that, as* $n \to \infty$, $R_{ww}(n) \sim C_{\tau,\theta}\left\{n^{1-1/(\tau\theta)}\right\}$.

3.3. The Logarithmic map

The asymptotic behaviour of the correlations for this class of maps has been studied by several authors. The following theorem may be deduced from the work of Gouëzel (2004a).

Theorem 3.3. (a) *For the Logarithmic map defined by* (18),

$$R_{ww}(n) = \frac{\eta_w^2 \chi_\beta(\frac{1}{2})}{2\beta(\log n)^\beta} + o\bigg(\frac{1}{(\log n)^\beta}\bigg),$$

where $\chi_\beta(w)$ *denotes the invariant density of the map and* $\eta_w = E(w_t)$ *for all* t.

(b) *For the generalized polynomial-logarithmic map defined by* (18),

$$R_{ww}(n) = M(\gamma)L^*(n)n^{1-\frac{1}{\gamma}} + o(L^*(n)n^{1-\frac{1}{\gamma}}),$$

where $M(\gamma)$ *is a constant and* $L^*(n)$ *is a slowly varying function at infinity.*

4. Small Frequency Analysis of the Spectral Density Function

Based on the results given in Section 3, the limiting behaviour of the spectral density function $f_{ww}(\lambda)$ as $\lambda \to 0$ may be investigated by appealing to classical Fourier Analysis, see (Zygmund, 1988, Chap. V). We distinguish between the following scenarios, in which $B > 0$ denotes a constant, though not necessarily the same constant each time; also, for convenience, we write $r(n)$ for $r_{ww}(n)$ and consider the normalized spectral density, $\overline{f}(\lambda) = f_{ww}(\lambda)/R_{ww}(0)$:

Scenario 1: The correlations decrease to 0 at a polynomial rate:

$$r(n) \sim Bn^{-\kappa} \quad \text{as } n \to \infty,\ 0 < \kappa < \infty,\ \kappa \neq 1; \tag{23}$$

Scenario 2: The correlations decrease to 0 like an harmonic sequence:

$$r(n) \sim Bn^{-1}, \quad (n \to \infty); \tag{24}$$

Scenario 3: The correlations decrease to 0 at a logarithmic rate:

$$r(n) \sim B(\log n)^{-\beta}, \quad \text{as } n \to \infty,\ 0 < \beta < \infty; \tag{25}$$

Scenario 4: The correlations decrease to 0 as follows:

$$r(n) \sim B\Delta(n)n^{2d-1}, \quad (n \to \infty), \tag{26}$$

where $d \in (-\infty, 0.5]$ and $\Delta(n)$ is a slowly varying function at ∞.

Note that Scenario 4 encompasses Scenarios 1, 2 and 3.

It follows from (22) that, with $\kappa = \alpha^{-1} - 1$, $\alpha \in (0,1)$, the Polynomial map generates correlations according to Scenario 1 provided $\alpha \neq 0.5$; moreover, part (c) of Theorem 3.2 shows that for $\kappa = (\tau\theta)^{-1} - 1$, $\tau\theta \in (0,1)$, the correlations of the extended symmetric cusp map also accord with this scenario. Similarly, Theorem 3.1 shows that the correlations of symmetric cusp map follow Scenario 2 with $B = 2$; in addition, by (22), the correlations of the Polynomial map with $\alpha = 0.5$ also follow this scenario. Finally, Theorem 3.3 shows that Scenario 3 holds for the Logarithmic map and Scenario 4 for the generalised Polynomial-Logarithmic map.

The various intermittency maps may thus be applied for generating realizations whose correlations follow Scenarios 1−4 outlined above and, also, for investigating the efficacy of various statistical methods for estimating the long-memory parameter under these scenarios. It should nevertheless be observed that the value of B, the multiplying constant, in these scenarios is known only for the symmetric cusp map, since a closed-form expression for its invariant density is given at (15). Exact analytic expressions for the invariant densities of the remaining maps are as yet unavailable, and hence the relevant value of B for these maps is also unknown.

It is readily checked, see Beran (1998), that under Scenario 1, the spectral density is given by (4) with $d = (1-\kappa)/2$. Scenarios 2 and 3 have hitherto not been considered in the literature and, see Section 1, they represent the two boundary points of the values of d specified by (2). Theorems 4.1 and 4.2. below give the asymptotics of the normalized spectral density function for these two scenarios, as $\lambda \to 0$, and Theorem 4.3 does the same for Scenario 4.

Theorem 4.1. *If Scenario 2 holds, the normalized spectral density function has the form*

$$\overline{f}(\lambda) = f^*(\lambda) \log \left| 2\sin(\frac{\lambda}{2}) \right| \tag{27}$$

as $\lambda \to 0$, where f^* is a function that is bounded away from zero and infinity, and $f^*(\lambda) \to -B\pi^{-1}$ as $\lambda \to 0$.

Proof. We have, see Zygmund (1988), that

$$\sum_{n\geq 1} \frac{1}{n} \cos n\lambda = -\log \left| 2\sin(\frac{\lambda}{2}) \right|.$$

Also, for a fixed, arbitrary $\epsilon > 0$, there exists an $N > 0$ such that $|B^{-1}nr(n) - 1| < \epsilon$ for all $n \geq N$. Moreover, for this N, there exists a $\lambda_N > 0$ such that $-\epsilon \log|2\sin(\lambda/2)| > 2\pi N$ for any $|\lambda| < \lambda_N$. Hence, for the given choice of N we have, for all $|\lambda| < \lambda_N$,

$$\overline{f}(\lambda) \leq -\frac{B}{\pi}(1+2\epsilon) \log \left| 2\sin(\frac{\lambda}{2}) \right|.$$

Similarly for the same choice of ϵ and $|\lambda| < \lambda_N$, we have

$$\overline{f}(\lambda) \geq -\frac{B}{\pi}(1-2\epsilon)\log\left|2\sin(\frac{\lambda}{2})\right|.$$

Since $\epsilon > 0$ is arbitrary the conclusion of the theorem follows.

Theorem 4.2. *If Scenario* 3 *holds, the normalized spectral density function,* $\overline{f}(\lambda)$*, has the form,*

$$\overline{f}(\lambda) = \frac{f^*_\beta(\lambda)}{\lambda}\Big(\log(\frac{1}{\lambda})\Big)^{1+\beta} \tag{28}$$

as $\lambda \to 0$*, where* f^*_β *is a continuous function that is bounded away from zero and infinity.*

Proof. It can be shown that, see Zygmund (1988, Theorem 2.17),

$$\sum_{n\geq 2}\frac{\cos n\lambda}{(\log n)^\beta} \sim \frac{\beta\pi}{2\lambda}\Big(\log(\frac{1}{\lambda})\Big)^{1+\beta} \qquad (\lambda \to 0).$$

Arguing in the same way as in the proof of Theorem 4.1, the required expression for $\overline{f}$ follows.

The following theorem generalizes Theorems 4.1 and 4.2; its proof follows from a result in Zygmund (1988, p.187), and is omitted.

Theorem 4.3. *If Scenario* 4 *holds, the normalized spectral density function has the form*

$$\overline{f}(\lambda) = |\lambda|^{-2d}\tilde{\Delta}(\frac{1}{\lambda}) \tag{29}$$

as $\lambda \to 0$*, where* $\tilde{\Delta}$ *is a slowly varying function at infinity.*

5. An Analysis of the Periodogram for Long Memory Map Time Series

Given a (part) realisation, w_t, $t = 0, \ldots, T-1$, of a weakly stationary process $\{w_t\}$, the sample autocovariance function is defined by

$$R_T(u) = \frac{1}{T}\sum_{t=0}^{T-u-1}(w_t - \overline{w}_T)(w_{t+u} - \overline{w}_T), \qquad \overline{w}_T = \frac{1}{T}\sum_{t=0}^{T-1} w_t, \tag{30}$$

and, with $\lambda = \lambda_j = 2\pi j/T$, the periodogram function by

$$I_T(\lambda) = \frac{1}{2\pi T}\Big|\sum_{t=0}^{T-1}(w_t - \overline{w}_T)e^{-i\lambda t}\Big|^2 = \frac{1}{2\pi}[R_T(0) + 2\sum_{j=1}^{T-1} R_T(j)\cos(j\lambda)]. \tag{31}$$

The periodogram is a basic statistic for estimating the memory parameter, d, of a long memory process, see Robinson (1995). If $\{w_t\}$ is a weakly stationary process and the mean $\eta = \mathbb{E}(w_t)$ is known, the expectation of the periodogram is given by, see Hurvich and Beltrao (1993),

$$\mathbb{E}\{I_T(\lambda)\} = \int_{-\pi}^{\pi} \frac{1}{T} \left(\frac{\sin(\frac{T(\lambda-\theta)}{2})}{\sin(\frac{\lambda-\theta}{2})} \right)^2 f(\theta)\, d\theta. \tag{32}$$

On the assumption that (2) holds, Hurvich and Beltrao (1993) but see also Robinson (1995), study the asymptotic bias

$$L_j = \lim_{T\to\infty} \mathbb{E}\left(\frac{I_T(\lambda_j)}{f(\lambda_j)} \right), \tag{33}$$

and show that

$$L_j = L_j(d) = \frac{2}{\pi} \int_{-\infty}^{\infty} \frac{\sin^2(\frac{x}{2})}{(2\pi j - x)^2} \left| \frac{x}{2\pi j} \right|^{-2d} dx. \tag{34}$$

These authors also investigate the various properties of $L_j(d)$ as a function of d, and show that $L_j(0) = 1$. Note that our Scenario 1 is equivalent to requiring that (2) holds.

Below, we study the asymptotic bias of the periodogram under Scenarios 2, 3 and 4. We show in particular that under Scenario 2, $L_j = 1$ and $\mathbb{E}\left(I_T(\lambda_j)\right) \to f(\lambda_j)$, as $T \to \infty$, for each fixed j. This last result implies that there exists a long memory process with slowly-decaying correlations for which the asymptotic unbiasedness property of the periodogram holds.

Theorem 5.1. *Suppose that Scenario 2 holds. Then*

$$L_j = \lim_{T\to\infty} \mathbb{E}\left(\frac{I_T(\lambda_j)}{f(\lambda_j)} \right) = \frac{2}{\pi} \int_{-\infty}^{\infty} \frac{\sin^2(x/2)}{(2\pi j - x)^2}\, dx = L_j(0) = 1.$$

Proof. We follow Hurvich and Beltrao (1993). Let $g_T(x) = F_T(\lambda_j - x) f(x) f(\lambda_j)^{-1}$. We have

$$L_j = \lim_{T\to\infty} \mathbb{E}\left(\frac{I_T(\lambda_j)}{f(\lambda_j)} \right) = \lim_{T\to\infty} \int_{-\pi}^{\pi} g_T(x)\, dx.$$

For a suitable $\delta \in (0,1)$, let

$$J_T = \int_{-T^{-\delta}}^{T^{\delta}} g_T(x)\, dx. \tag{35}$$

From the spectral representation of $g(x)$ we can show that that $J_T \to L_j$ as $T \to \infty$. The proof is now completed by demonstrating that

$$\lim_{T\to\infty} J_T = \frac{2}{\pi}\int_{-\infty}^{\infty} \frac{\sin^2(\frac{z}{2})}{(2\pi j - z)^2}\, dz = L_j(0) = 1.$$

Theorem 5.2. *Suppose that Scenario* 3 *holds. Then*

$$L_j = \lim_{T\to\infty} \mathbb{E}\left(\frac{I_T(\lambda_j)}{f(\lambda_j)}\right) = \frac{2}{\pi}\int_{-\infty}^{\infty} \frac{\sin^2(\frac{x}{2})}{(2\pi j - x)^2}\left|\frac{x}{2\pi j}\right|^{-1} dx = L_j(\frac{1}{2}).$$

Proof. The method of proof is similar to that for Theorem 5.1, but we now have

$$\lim_{T\to\infty} J_T = 4j\int_{-\infty}^{\infty} \frac{\sin^2(\frac{x}{2})}{x(2\pi j - x)^2}\, dx = L_j(\frac{1}{2}). \tag{36}$$

Theorem 5.3. *Suppose that Scenario* 4 *holds. If, in addition, there exists a* $\delta \in (0, 0.5)$ *such that for each* j,

$$\lim_{T\to\infty} \int_{-T^{1-\delta}}^{T^{\delta}} \left\{\frac{\tilde{\Delta}(\frac{T}{x})}{\tilde{\Delta}(\frac{1}{\lambda_j})} - 1\right\} \frac{\sin^2(\frac{x}{2})}{(2\pi j - x)^2}\left|\frac{x}{2\pi j}\right|^{-2d} dx = 0,$$

then

$$L_j = \lim_{T\to\infty} \mathbb{E}\left(\frac{I_T(\lambda_j)}{f(\lambda_j)}\right) = \frac{2}{\pi}\int_{-\infty}^{\infty} \frac{\sin^2(\frac{x}{2})}{(2\pi j - x)^2}\left|\frac{x}{2\pi j}\right|^{-2d} dx = L_j(d).$$

Remark 5.4. If $\{w_t\}$ is generated by a deterministic map ζ so that $w_t = \zeta^t(w_0)$, Theorems 5.1, 5.2 and 5.3 apply to this map time series provided ζ is ergodic and w_0 is a realization of the invariant distribution of the map.

6. Simulation Results

We investigate the extent to which the asymptotic result on the rate of decay of correlations for the symmetric cusp map applies with simulated realizations of T consecutive observations from this map. In addition, we examine the low-frequency behaviour of the estimated spectral density functions of the polynomial, logarithmic and symmetric cusp maps. We also consider the autoregressive spectral estimate. For a linear process admitting an infinite autoregressive representation, Berk (1974) shows that the autoregressive spectral estimate is asymptotically equivalent to a smooth periodogram estimate of the spectral density. Their relative sampling properties for simulated series of finite length

are examined by Beamish and Priestley (1981) and Bhansali (1997), among others. By contrast, however, much of the current 'long-memory' literature has focussed on the periodogram and little is currently known, either theoretically or empirically, about the properties of the autoregressive spectral estimate for this class of processes. Moreover we consider non-linear chaotic maps, and the simulations should provide further information on their relative performance in this situation.

A motivation underpinning the simulation study is that the existing statistical explanations for the long-memory phenomenon are based on the notion of aggregation, see Park and Willinger (2000), among others. The intermittency maps considered in this paper provide a different physical explanation of how long memory could arise, namely through their recurrence properties and the rather long periods the orbit could spend in the laminar region, close to the neutral fixed point. At the same time, however, the ergodic results only show that the various 'time averages' converge to the corresponding 'ensemble averages' as the number of observations over which the time averages are taken grows indefinitely. An estimate of the rate at which the convergence occurs is as yet unavailable. It is hoped that the simulation study can help to bridge the gulf between mathematical dynamical systems theory and a practical verification of its asymptotic results with generated series of moderately large length.

6.1. Plan of the study

A stretch of $N = 10^7$ iterations of the polynomial, logarithmic and symmetric cusp maps was generated, but only the last $T = 10^4$ observations, $\{w_t, t = M + 1, \ldots, M + T\}$, with $M = 10^7 - 10^4$, were actually retained for estimating the correlations, spectral density and related statistics, and the first M values were discarded; a 'burn-in' period of similar length was earlier adopted in Bhansali, Holland and Kokoszka (2006).

Let u_0 be uniform(0, 1). The initial value of the symmetric cusp map was:

$$w_0 = -1 + 2(1 - u_0)^{\frac{1}{2}}. \tag{37}$$

The initial value, w_0, for the polynomial and logarithmic maps was generated, see Bhansali, Holland and Kokoszka (2006), from an exponential distribution with mean 0.2, truncated at 1.0. We set $\alpha = 0.4, 0.5, 0.667$ and $\beta = 0.05, 0.2, 0.35$. The NAG routines $G05DAF$ and $G05FBF$ were used for generating the uniform and exponential random numbers. The correlations, $r^{(T)}(u)$ $(u = 1, \ldots, 300)$, were computed as follows:

$$r^{(T)}(u) = \frac{R_T(u)}{R_T(0)}, \tag{38}$$

where $R_T(u)$ is defined at (30). The associated estimated partial correlations, $\hat{\pi}(k)$, $(k = 1, \ldots, 50)$, were then computed by the NAG routine $G13ACF$ in accordance with the Durbin-Levinson algorithm. The order of an appropriate linear autoregressive approximation was also determined by minimising the BIC criterion:

$$BIC(k) = T \log \hat{\sigma}^2(k) + (\log T)k \qquad (k = 0, \ldots, 50), \tag{39}$$

with $\hat{\sigma}^2(k) = \hat{\sigma}^2(k-1)\{1 - \hat{\pi}^2(k)\}$, $\hat{\sigma}^2(0) = R_T(0)$. An autoregressive model of order $k = \hat{k}$, where $\hat{k}$ denotes the value of k selected by the BIC criterion, was fitted by the NAG maximum likelihood routine $G13AFF$; the goodness of the fitted model was tested by the NAG routine $G13ASF$. An autoregressive spectral estimate, $\hat{f}_k$ was computed as

$$\hat{f}_k(\lambda) = \frac{\hat{\sigma}^2(k)}{2\pi} |\hat{A}_k(\lambda)|^{-2}, \tag{40}$$

where

$$\hat{A}_k(\lambda) = \sum_{u=0}^{k} \hat{a}_k(u) \exp(iu\lambda), \qquad \hat{a}_k(0) = 1, \tag{41}$$

denotes the estimated autoregressive transfer function and the $\hat{a}_k$ denote the maximum likelihood estimates of the autoregressive coefficients.

A NAG fast Fourier routine, $C06ECF$, was applied for computing the periodogram I_T and the autoregressive transfer function $\hat{A}_k(\lambda)$, for $\lambda = \tilde{\lambda}_j = (2\pi j)/2T$, $j = 0, \ldots, T-1$; moreover, the estimated covariances R_T were computed by an inverse Fourier transform of the periodogram. The normalized periodogram, $\overline{I}_T(\lambda) = I_T(\lambda)/R_T(0)$, and the normalized autoregressive spectral estimate, $\overline{f}_k(\lambda) = \hat{f}_k(\lambda)/R_T(0)$, were then computed.

The simulated sampling means, variances and standard deviations (SD) of the various estimates were determined by replicating the computations described above $NRP = 1,000$ times, and with a different initial condition each time. In addition, the simulated sampling distributions of $r^{(T)}(u)$, $u = 1, 2, 3$, $\hat{a}_k(1)$, $\bar{w}$, $R_T(0)$ and $\hat{k}$, the autoregressive order selected by the BIC criterion, were obtained, as were the histograms of the retained orbits $w_t\,(t = 1, \ldots, 10,000)$ for the first two replications of each map. There were, however, Q replications for which the NAG routine $G13ASF$ failed to converge. The numerical value of Q varied in [0, 55], the larger values occurring for the logarithmic map with $\beta = 0.05, 0.2$, and smaller values with other maps; moreover, there were some maps, for example the polynomial maps with $\alpha = 0.4, 0.5$, for which Q was 0. As the asymptotic results discussed in Sections 2 and 3 do not apply to these replications, it was decided to exclude them from our simulation study.

Nevertheless, for ensuring that the reported results were uniformly based on $1,000$ replications, the value of NRP was increased to $1,000 + Q$.

To save space, we present detailed results only for the symmetric cusp map. For the polynomial and logarithmic maps, we only consider the simulated sampling means of the normalized periodogram and the autoregressive spectral estimate; see Bhansali, Holland and Kokoszka (2006), however, for a discussion of the 'time domain' results for the sample correlations and related statistics for these maps.

6.2. The Symmetric cusp map

A histogram of $T = 10,000$ consecutive observations generated from this map with $w_0 = -0.09473545285$ is shown in Figure 1a, together with the corresponding triangular invariant density. The latter is given at (15), see Balakrishnan, Nicolis and Nicolis (1997); also, the histogram shown in Figure 1a is one with 25 class intervals, each of width 0.08. Apart from the first two class intervals close

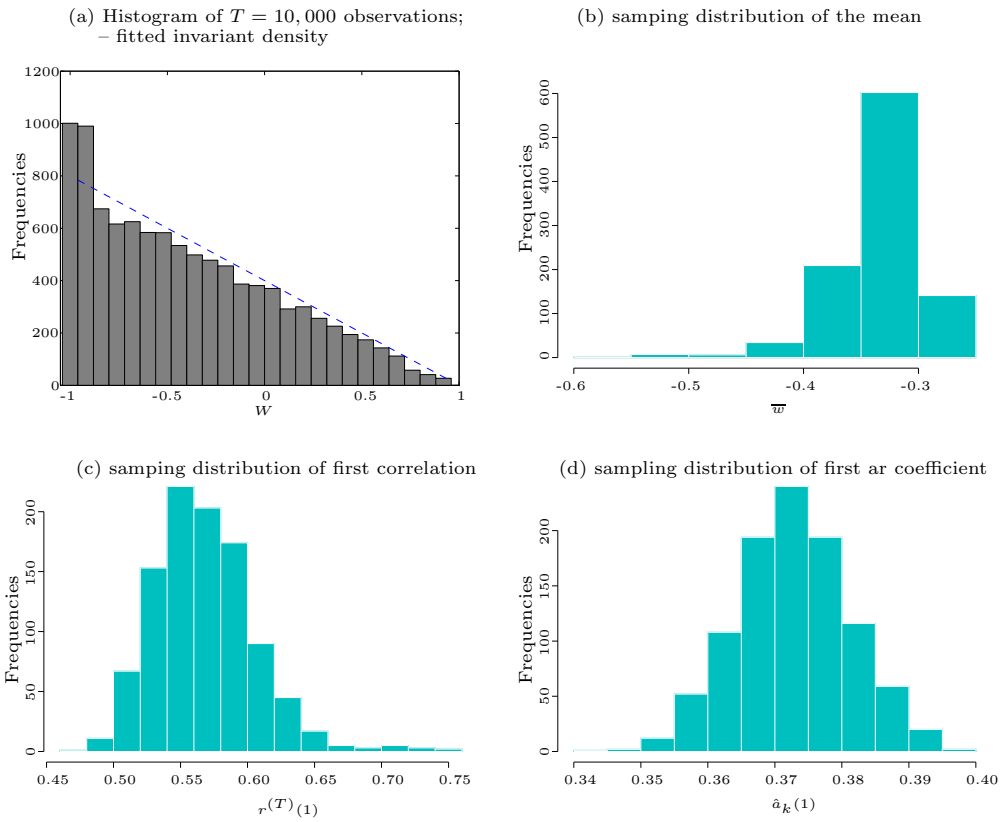

Figure 1. Histograms for the symmetric cusp map.

to -1.0, the neutral fixed point, the shape of the rest of the histogram accords with that of the triangular invariant density, though the relative frequencies of observations falling in the corresponding intervals are consistently overestimated. The relative frequency of the orbit remaining close to the neutral fixed point is underestimated by the invariant density.

A $P-P$ plot, which gets around grouping into class intervals, was obtained and is shown in Figure 2, together with the corresponding 45° line. Apart from the quantiles near -1.0, or 1.0, the $P-P$ plot is close to the 45° line, indicating that the invariant density provides a reasonably good fit for the simulated observations in the middle-part of the distribution.

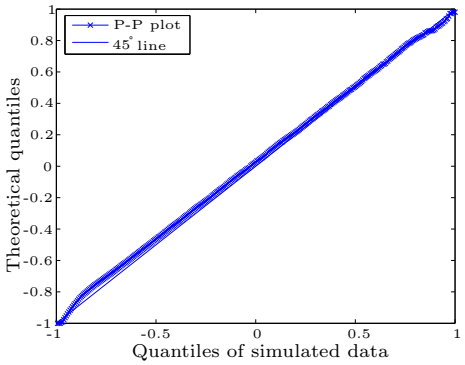

Figure 2. P-P plot for the symmetric cusp map.

Figures 1b and 1c show the histograms of the sampling distributions of the mean $\overline{w}$ and the first correlation $r^{(T)}(1)$. The former is centered around the corresponding theoretical value, $\eta = E(w) = -1/3$, in fact the sampling mean was -0.33418, and the latter around $r_{ww}(1) = 0.571$. Both histograms display a tail behaviour: the histogram of the mean is left-skewed and contains some very small values; that of $r^{(T)}(1)$ is right-skewed and contains some large values. The latter feature was also evident in the histograms of the sampling distributions of $r^{(T)}(2)$ and $r^{(T)}(3)$, not shown here. This tail behaviour is further exacerbated if the results for the discarded $Q = 10$ replications are included in the simulation study, see the discussion in Section 6.1.

Figures 3a and 3b show plots of the simulated means of the sample correlations, $r^{(T)}(u)(u = 1, \ldots, 300)$ and partial correlations, $\hat{\pi}(k)$ $(k = 1, \ldots, 50)$, together with two curves representing mean+SD and mean-SD. The mean correlations decrease more slowly than the theoretical asymptotic rate given in Theorem 3.1. The numerical magnitude of the standard deviation, SD, is, however, relatively large at high lags u, and it remains approximately constant as u increases. Hence, it is not feasible to draw meaningful conclusions concerning the

extent to which the simulation results support the asymptotic theory. Although the first few values of the mean partial correlations dominate the rest of the values, the mean - SD curve is above 0 for all $u < 15$, indicating that a relatively high order may be needed for developing a linear autoregressive approximation for the map from only a finite realization of the corresponding time series. An inspection of the frequency distributions of the autoregressive order selected by the BIC criterion revealed that, whereas the average autoregressive order selected for this map was 8.02, and for the polynomial map with $\alpha = 0.5$, was 3.84, the percentiles of the distributions of the autoregressive order selected for the former map are higher than those for the latter map although they have the same asymptotic decay of correlations. Figure 1d shows the histogram of $\hat{a}_k(1)$, with $k = \hat{k}$, the autoregressive order selected by the BIC criterion, for the symmetric cusp map. The histogram is almost symmetric and close in shape to the density function of a Normal distribution, suggesting that the maximum likelihood estimates of the autoregressive coefficients are well-behaved for this map.

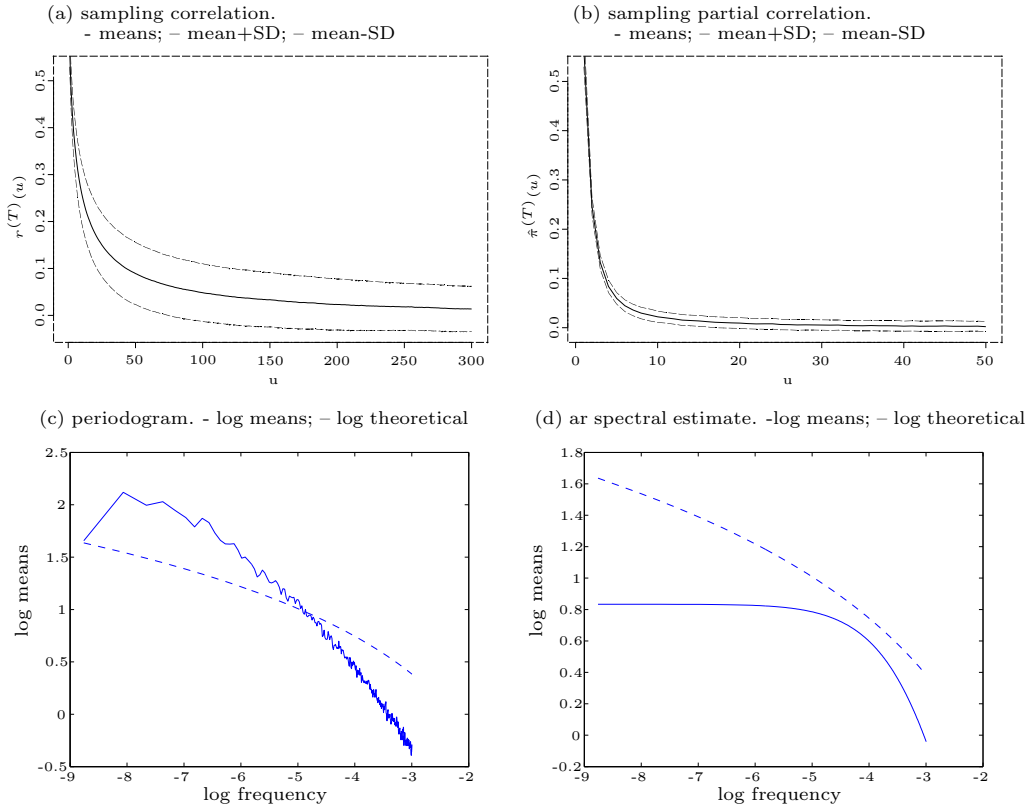

Figure 3. Means for the symmetric cusp map.

A plot of the logarithm of the simulated means of the normalized periodogram $\overline{I}_T(\lambda_j)$ against the logarithm of frequency for $\tilde{\lambda}_j = j\pi/T, j = 1, \ldots, 316$, is shown in Figure 3c, together with the logarithm of the corresponding theoretical spectral density, $\overline{f}$; the latter was computed from (27). Figure 3d shows the same information for the normalized autoregressive spectral estimate $\overline{f}_k$. By Theorem 5.1, the periodogram provides an asymptotically unbiased estimator of the spectral density function of this map, as $T \to \infty$. The simulation results in Figure 3c are partially in agreement with this theoretical result, since the overall shape of the simulated means accords with that of the theoretical spectrum. The numerical values of the simulated means differ considerably from the corresponding theoretical values however, indicating a substantial bias with finite-length realizations generated from the map. A slight dip in the mean periodogram for the two frequencies closest to the origin arises because the periodogram was computed by subtracting the sample mean $\overline{w}$ from each w_t, thus treating the mean, $\eta = E(w_t)$, as unknown. Since the latter is known, the periodogram was also recomputed from the realization $\tilde{w}_t = w_t + 1/3$. To save space, the corresponding simulated means are not shown here. Suffice it to say that, away from the origin, these new means differ little from those shown in Figure 2c, but at the two frequencies closest to the origin, the dip visible in this figure disappears and the new means follow the same overall shape as that at other low frequencies.

By Theorem 4.1, $d = 0$ for this map. It may, however, be gleaned from Figure 3c that a log-log plot of the simulated means of the periodogram is quite linear in a neighbourhood of the zero frequency and, if d is estimated by a log-periodogram regression, this estimate could be badly biased upwards. A log-log plot of the simulated means of the autoregressive spectral estimate is, however, quite flat for small frequencies and its appearance is consistent with the theoretical value of $d = 0$. On the other hand, the autoregressive spectral estimate is numerically not as close to the theoretical spectrum as the periodogram, and its functional shape is also quite different from that of the theoretical spectrum.

6.3. The polynomial and logarithmic maps

Figures 4a and 4b show the means of the periodogram and the autoregressive spectral estimate for $\alpha = 0.5$. Apart from a multiplying constant, Theorem 4.1 also applies to this map and shows that in a neighbourhood of the origin, the theoretical spectrum of this map and that of the symmetric cusp map are given by (4.1). Nevertheless, the relevant multiplying constant for the former map is, as yet, unknown, and therefore, unlike Figures 3c and 3d, the corresponding theoretical spectrum is not shown in Figures 4a and 4b. The simulation results partially agree with the asymptotic theory, since the simulated means shown in Figures 4a and 4b and those shown in Figures 3c and 3d have similar shapes.

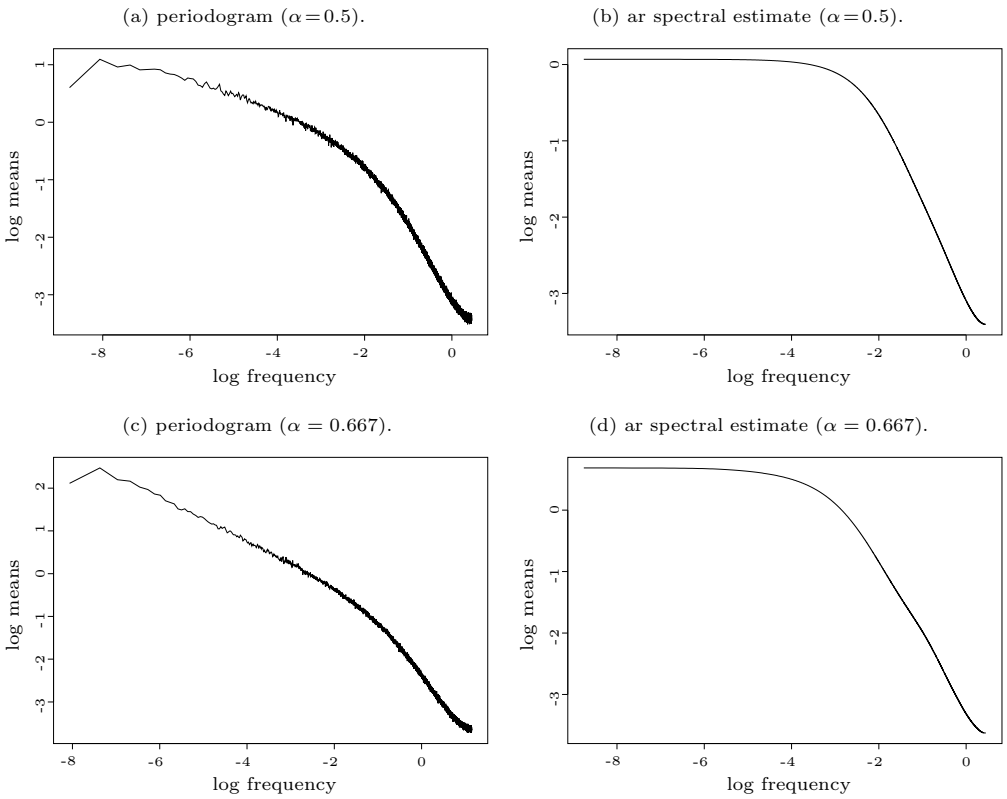

Figure 4. Simulated means for the polynomial map.

As may be gleaned from Figure 4c, for $\alpha = 0.667$ the simulation results for the periodogram broadly accord with the asymptotic theory, and in a neighbourhood of the origin a log-log plot of their simulated means decreases linearly. This is not so, however, for the autoregressive estimate, since Figure 4d shows that its behaviour with $\alpha = 0.667$ is quite similar to that for $\alpha = 0.5$.

For $\alpha = 0.4$, the asymptotic theory shows that the theoretical spectral density should increase with the frequency. The simulated means of the periodogram and the autoregressive spectral estimate decrease as the frequency increases however, and thus their behaviour is not as sensitive to the choice of α as implied by the asymptotic theory. To save space, the corresponding plots are omitted.

Theorem 4.2 shows that, for small frequencies, the spectral density $\log f_\beta$ of the logarithmic map is dominated by a linear function of $\log(\lambda)$, whose slope of -1 does not depend upon the parameter β. The corresponding simulated means of the periodogram and autoregressive spectral estimate are shown in Figures 5a to 5f with $\beta = 0.05$ and 0.2. Although the former do appear linear, the slopes of the fitted regression lines depend upon the value of β, and numerically estimated slopes calculated from the mean-periodogram are consistently less than

the asymptotic value. For frequencies very close to the origin, the autoregressive spectral estimate is more curved than either the periodogram or the corresponding autoregressive estimates shown in Figures 3 and 4 for the symmetric cusp and polynomial maps. It is however possible to identify, see Figures 5e and 5f, a

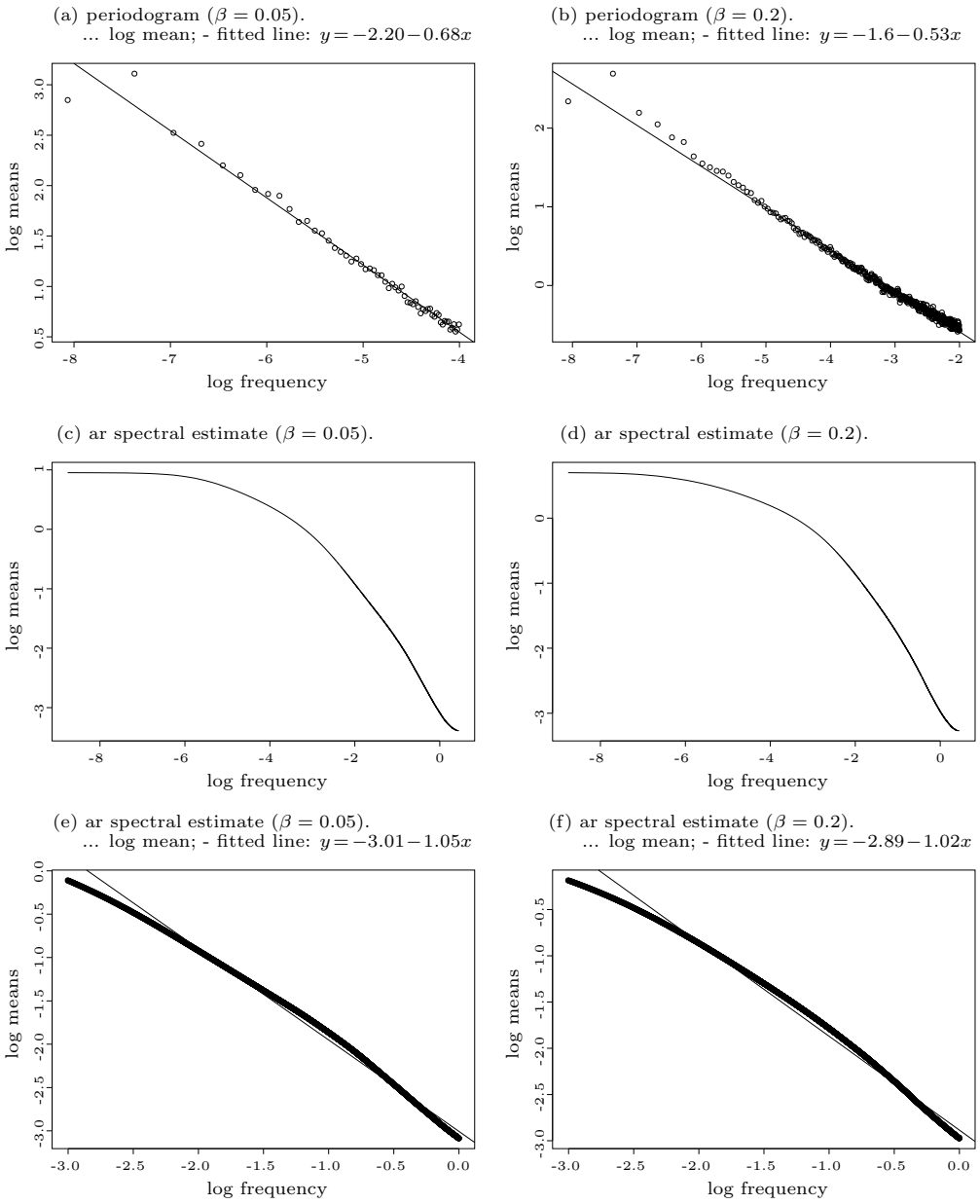

Figure 5. Means for the logarithmic map.

band of small frequencies, somewhat away from the origin, where this estimate is almost linear. The estimated slope, while closer to the asymptotic value than that for the periodogram, still depends upon the value of β. The corresponding results with $\beta = 0.35$ are not shown, to save space,. Suffice it to say, however, that the estimated slope with the autoregressive spectral estimate is now -0.76, indicating that even when the band of frequencies for estimating the memory parameter from an autoregressive spectral estimate is carefully chosen, the relative agreement between the asymptotic theory and simulation results decreases as β increases. Moreover the question of how to choose an appropriate frequency band for applying such a procedure requires further consideration.

6.4. Summary and Conclusions

For all three maps, the simulation results only partially agree with the asymptotic theory. The disparity in the case of the symmetric cusp map could be attributed to the relative preponderance of simulated observations near the neutral fixed point than predicted by the asymptotic theory. The estimate of the memory parameter d obtained from the autoregressive spectral estimate appears closer to the theoretical value for both the symmetric cusp and polynomial map with $\alpha = 0.5$, i.e., at the lower boundary of the interval, $[0.0, 0.5]$ than that from the periodogram. The converse however holds for the polynomial map where the estimate of d obtained from the former is not as sensitive to the choice of α as the latter. This may be because the shape of the autoregressive estimate depends upon the properties of the fitted autoregressive model and less directly on that of the underlying theoretical spectrum, see Beamish and Priestley (1981). For the logarithmic map, whose memory parameter falls at the upper boundary of the interval $[0.0, 0.5]$, it is possible to identify a narrow band of small frequencies where the logarithm of the mean of autoregressive spectral estimate is almost linear and the slope of the fitted line is closer to the corresponding theoretical value than that for the periodogram. This observation, however, raises the question of how to choose an appropriate frequency band for estimating the memory parameter from an autoregressive spectral estimate, and requires further investigation; moreover, a similar difficulty applies also to the well-known GPH and related non-parametric and semi-parametric methods of estimating the memory parameter from the periodogram. A surprising finding of the simulations is the approximate normality of the estimated autoregressive coefficient for the symmetric cusp map. A similar result was noticed also for the polynomial and logarithmic maps, suggesting that the classical result on the asymptotic normality of the maximum likelihood estimates of the autoregressive parameters could also apply more generally to time series generated by intermittency maps.

Acknowledgements

M. Holland acknowledges the support of an EPSRC research grant, no. GR/S11862/01. Thanks are also due Mr. Lan Yang and Mr. Dilbag Sokhi of Liverpool University for their help in producing the graphs included in this paper.

Appendix: Proof of Theorem 3.1

Following Young (1999), we analyse the recurrence time statistics of the symmetric cusp map $\zeta(w)$. The idea is as follows: choose a set $Y \subset J$, and consider the first return map $\widetilde{T}(w) : Y \to Y$, where $\widetilde{T}(w) = \zeta^{R(w)}(w)$, and $R(w) = \inf\{n \geq 0 : \zeta^n(w) \in Y\}$. Partition Y into subsets $\{Y_i\}$ such that $R \mid_{Y_i} = R_i$ is constant, and $\widetilde{T}(Y_i) = Y$ with bounded distortion on the derivatives of $\widetilde{T} \mid_{Y_i}$. An estimate of the tail of the return times, namely the quantity $\mu\{w \in Y : R(w) > n\}$ can be used to estimate the rate of decay of correlations. Here μ is the invariant measure of $\zeta(w)$ with density $\chi_S(w)$. In particular a result of Gouëzel (2004a) is used to infer that the correlations behave asymptotically as $\sum_{k \geq n} \mu\{w \in Y : R(w) > n\}$, up to a known multiplication constant. For the symmetric cusp map we show that this latter quantity decays like $\mathcal{O}(1/n)$.

For an appropriate subinterval Y, we construct the partition $\{Y_i\}$ of Y, and show that the return time function $R(w)$ has the appropriate asymptotics.

Let $Y^r = [0, p]$, where p is the (hyperbolic repelling) fixed point of T, namely the point $p > 0$ such that $p = 1 - 2\sqrt{p}$. Let $Y^l = [-p, 0]$, and note that $\zeta(-p) = p$. We now identify subsets $Y_n^r \subset Y^r$ and $Y_n^l \subset Y^l$ such that $\zeta^k(Y_n^l), \zeta^k(Y_n^r)$ are disjoint from $Y^l \cup Y^r$ for $k = 1, \ldots, n-1$, and $\zeta^n(Y_n^r), \zeta^n(Y_n^l) = Y^l \cup Y^r$ so that $R \mid_{Y_n^r}, R \mid_{Y_n^l} = n$. By construction, it will follow that the restriction of ζ^n to Y_n^l and Y_n^r has uniformly bounded distortion.

Lemma 6.1. *The sets Y_n^l, Y_n^r have the form $Y_n^l = [-y_n, -y_{n+1}], Y_n^r = [y_{n+1}, y_n]$, where $y_n \sim n^{-2}$. Moreover $\mu\{R > n\} \sim n^{-1}$, where R is the first return time function to $Y^l \cup Y^r$, and $R \mid Y_n^l, R \mid Y_n^r = n$.*

The proof of this lemma goes as follows. Let $w_n = \zeta^{-n}(p) \cap [-1, 0]$, so that $w_n \to -1$ as $n \to \infty$. An elementary argument (see Holland (2005) for example) shows that $w_n + 1 \sim 2n^{-1}$. Under the map ζ, the intervals Y^r, Y^l each map onto $[p, 1]$, and therefore T^2 maps each of Y^r, Y^l bijectively onto $[-1, p]$. Hence the intervals Y_n^r, Y_n^l correspond to intervals which map to $[w_{n-1}, w_{n-2}]$ under $\zeta^2(w)$. For $w > 0$, $\zeta^{-1}(w) = (1-w)^2/4$, and

$$y_n = \zeta^{-2}(w_{n-2}) = \frac{1}{4}\big(1 - \frac{1}{4}(1 - w_{n-2})^2\big)^2 \sim \frac{1}{n^2}$$

as $n \to \infty$. Therefore $\mu\{R > n\} = \int_{-y_n}^{y_n} \chi_S(x)dx$ where $\chi_S(x) = (1-x)/2$, and we obtain $\mu\{R > n\} = y_n \sim n^{-2}$.

The following lemma summarizes bounded distortion for $\zeta^n(w)$ on Y_n^l, Y_n^r. We do not give the proof as it follows from the techniques used in (Holland, 2005, Proposition 2).

Lemma 6.2. *There exists a constant $D > 0$ independent of n, such that for all Y_n^l, Y_n^r and $w \in Y_n^l \cup Y_n^r$ we have*

$$\frac{|(\zeta^n)''(w)|}{(\zeta^n)'(w)^2} \leq D. \tag{42}$$

From the return time asymptotics and bounded distortion we now use the result of Gouëzel (2004a) to obtain the correlations. The following estimate holds.

Proposition 6.3. *Let $\varphi(w)$ and $\psi(w)$ be two functions which tend to 0 at $w = -1$. Then*

$$\int \varphi(w)\psi(\zeta^n w)\chi_S(w)\,dw - \int \varphi(w)\chi_S(w)\,dw \int \psi(w)\chi_S(w)\,dw$$
$$= \Big(\sum_{k=n}^{\infty} \mu\{R > k\}\Big) \int \varphi(w)\chi_S(w)\,dw \int \psi(w)\rho(w)\,dw + o\Big(\sum_{k=n}^{\infty} \mu\{R > k\}\Big).$$

For a proof of Proposition 6.3 we refer to Gouëzel (2004a). To complete the proof of Theorem 3.1, we use Proposition 6.3 applied to the functions $\varphi(w) = \psi(w) = w + 1$. Notice that these functions vanish at $w = -1$. Moreover the correlation functions are unaffected by constant translation, and therefore

$$R_{w,w} = R_{w+1,w+1} = \frac{4}{9n} + o\left(\frac{1}{n}\right).$$

Remark 6.4. The corresponding result for the extended cusp, namely Theorem 3.2, is proved in a completely analogous way, we do not give the details.

References

Balakrishnan, V., Nicolis, G. and Nicolis, C. (1997). Recurrence time statistics in chaotic dynamics. I. Discrete time maps. *J. Statist. Phys.* **86**, 191-212.

Balakrishnan, V., Nicolis, G. and Nicolis, C. (2001). Recurrence time statistics in chaotic dynamics: multiple recurrences in intermittent chaos. *Stoch. Dyn.* **1**, 345-359.

Barndorff-Nielsen, O. E. (2001). Modelling by Levy Processes. In *Selected Proceedings of the Symposium on Inference for Stochastic Processes* (Edited by I. V. Basawa, C. C. Heyde and R. L. Taylor), 25-31. Institute of Mathematical Statistics, Beachwood, Ohio.

Beamish, N. and Priestley, M. B. (1981). A study of the autoregressive and window spectral estimation. *Appl. Statist.* **30**, 41-58.

Beran, J (1998). *Statistics for Long Memory Processes.* Chapman and Hall, London.

Berliner, L. M. (1992). Statistics, probability and chaos. *Statist. Sci.* **7**, 69-122.

Berk, K. N. (1974). Consistent autoregressive spectral estimates. *Ann. Statist.* **2**, 489-502.

Bhansali, R. J. (1997). Robustness of the autoregressive spectral estimate for linear processes with infinite variance. *J. Time Ser. Anal.* **18**, 213-229.

Bhansali, R. J. Holland, M. P. and Kokoszka, P. S. (2005). Chaotic maps with slowly decaying correlations and intermittency. In *Asymptotic Methods in Stochastics, Festschrift for Miklos Csorgo* **44** (Edited by L. Horvath and B. Szyszkowicz), 99-126. American Mathematical Society, Providence, RI.

Bhansali, R. J. Holland, M. P. and Kokoszka, P. S. (2006). Intermittency, long-memory and financial returns. In *Long Memory in Economics.* (Edit by G. Teysssiere and A. Kirman), 39-68. Springer, Berlin.

Box, G. E. P, Jenkins, G. M. and Reinsel, G. (1994). *Time Series Analysis: Forecasting and Control*. Holden Day, New York.

Doukhan, P. Oppenheim, G. and Taqqu, M. S. (2002). *Theory and Applications of Long-Range Dependence*. Birkhauser, Boston.

Frisch, U. (1996). *Turbulence: The Legacy of A. N. Kolmogorov.* Cambridge University Press, Cambridge, U.K.

Gao, J. Anh, V. Heyde, C. and Tieng, Q. (2001). Parameter estimation of stochastic processes with long- range dependence and intermittency *J. Time Ser. Anal.* **22**, 517-535.

Giraitis, L. and Taqqu, M. S. (1999). Whittle estimators for finite variance non-Gaussian time series with long memory. *Ann. Statist.* **27**, 178-203.

Gouëzel, S. (2004a). Vitesse de décorrélation et théorèmes limites pour les applications non uniformément dilatantes. Ph.D. Thesis, Ecole Normale Supérieure.

Gouëzel, S. (2004b). Sharp polynomial estimates for the decay of correlations. *Israel J. Math.* **139**, 29-65.

Holland, M. P. (2005). Slowly mixing systems and intermittency maps. *Ergodic Theory Dynam. Systems* **25**, 133-159.

Hurvich, C. and Beltrao, K. (1993). Asymptotics for the low-frequency ordinates of the periodogram of a long memory time series. *J. Time Ser. Anal.* **14**, 455-472.

Liverani, C. Saussol, B. and Vaienti, S. (1999). A probabilistic approach to intermittency. *Ergodic Theory Dynam. Systems* **19**, 671-685.

Martin, R. J. and Eccleston, J. A. (1992). A new model for slowly-decaying correlations. *Statist. Probab. Lett.* **13**, 139-145.

Martin, R. J. and Walker, A. M. (1997). A power-law model and other models for long-range dependence. *J. Appl. Probab.* **34**, 657-679.

Mcleod, A. I. (1998). Hyperbolic decay of time series. *J. Time Ser. Anal.* **19**, 473-484.

Park, K. and Willinger, W. (2000). *Self-Similar Network Traffic and Performance Evaluation.* John Wiley, New York.

Pronzato, L. Wynn, H. P. and Zhigliavsky, A. A. (2001). Analysis of performance of symmetric second-order line search algorithms through continued fractions. *IMA J. Math. Control Inform.* **18**, 281-296.

Rangarajan, G. and Ding, M. (2003). *Processes with Long-Range Correlations*. Springer, Berlin.

Robinson, P. M. (1995). Log-periodogram regression of time series with long range dependence. *Ann. Statist.* **23**, 1048-1072.

Russell, K. G. and Eccleston, J. A. (1987). The construction of optimal incomplete block design when observations within a block are correlated. *Austral. J. Statist.* **29**, 293-302.

Sarig, O. M. (2002). Subexponential decay of correlations. *Invent. Math.* **150**, 629-653.

Schuster, H. G. and Just, W. (1999). *Deterministic Chaos*. Wiley, New York.

Young, L. S. (1999). Recurrence times and rates of mixing. *Israel J. Math.* **110**, 153-188.

Zygmund, A. (1988). *Trigonometric Series, Volume I* Cambridge University Press, Cambridge.

Department of Mathematical Sciences, University of Liverpool, Liverpool, L69 3BX, United Kingdom.

E-mail: sa17@liv.ac.uk

The School of Engineering, Computer Science and Mathematics, University of Exeter, Harrison Building, North Park Road, Exeter, EX4 4QF, United Kingdom.

E-mail: M.P.Holland@exeter.ac.uk

(Received June 2005; accepted April 2006)